Aquaculture 492 (2018) 226–236

Contents lists available at ScienceDirect

Aquaculture

journal homepage: www.elsevier.com/locate/aquaculture

An integrated genetic map based on EST-SNPs and QTL analysis of shell color traits in Pacific oyster *Crassostrea gigas*

Jiulong Wang[a], Qi Li[a,b,*], Xiaoxiao Zhong[a], Junlin Song[a], Lingfeng Kong[a], Hong Yu[a]

[a] Key Laboratory of Mariculture, Ministry of Education, Ocean University of China, 5 Yushan Road, Qingdao 266003, China
[b] Laboratory for Marine Fisheries Science and Food Production Processes, Qingdao National Laboratory for Marine Science and Technology, Wenhai Road, Qingdao 266237, China

ARTICLE INFO

Keywords:
Crassostrea gigas
Shell color
EST-SNP
Linkage map
Quantitative trait loci

ABSTRACT

Shell color polymorphism is common in nature for the marine mollusks. The Pacific oyster *Crassostrea gigas*, is widely cultured and one of the most economically important bivalve species with various shell color variants. Here, a total of 1061 single nucleotide polymorphism markers, developed from expressed sequence tags (EST-SNPs), were used to construct two genetic linkage maps based on reciprocal-cross between black shell and white shell oysters (MF-A and MF-B) respectively. The two separate linkage maps were combined into an integrated map spanning 947.31 cM in total length. The integrated map was composed of 351 EST-SNP markers distributing on 10 linkage groups, with an average interval of 2.78 cM between adjacent markers. For the MF-A, 11 quantitative trait loci (QTLs) for shell color traits and five QTLs for growth traits were detected, explaining 8.1%–13.8% (mean = 11.76%) and 10.4%–11.0% (mean = 10.66%) phenotypic variance respectively. For the MF-B, nine QTLs for shell color traits and eight QTLs for growth traits were detected, explaining 8.8%–21.7% (mean = 12.84%) and 8.4%–9.4% (mean = 8.88%) phenotypic variance respectively. QTLs clustering was found on the linkage group 2 of the MF-A and the linkage group 8 of the MF-B, and the QTLs showed that pleiotropism could affect at most three traits. Three shared-QTLs associated with shell color traits were identified on the integrated map, and one of them (qA-*a** 4) was significantly homologous to *C. gigas* calmodulin-like protein. The QTLs identified in the present study could be useful in finding candidate genes for the shell color and growth-related traits in future, and potentially applied to marker-assisted selection breeding programs for *C. gigas*.

1. Introduction

Color plays an important role in many aspects of our life. It is a key factor in the food choice by affecting taste thresholds, sweetness perception, food preference, pleasantness, and acceptability (Clydesdale, 1993). Then it could affect the price of food products to a certain extent. For the marine mollusks, shell color polymorphism is common in nature, which brings visual aesthetics and attracts great interest of naturalists and collectors for a long time (Comfort, 1951). The Pacific oyster *Crassostrea gigas* (Thunberg 1793), is natively distributed along the Pacific coast of Asia and has been introduced to many countries worldwide for aquaculture purpose (Mann, 1991; Orensanz et al., 2002). Now it is one of the most important marine economic species and its global production ranks first in the cultured aquatic animals (FAO, 2014). Just as consumers are willing to pay more for the rich red salmon fillets (Steine et al., 2005; Alfnes et al., 2006), oysters with beautiful and pure shell and mantle color are popular in market and traded at a higher price (Nell, 2001; Kang et al., 2013). The shell pigmentation has aroused considerable interest in the oyster industry and it is considered as new potential phenotypic trait for improving commercial value (Ward et al., 2000; Brake et al., 2004; Kang et al., 2013).

In the past decades, a lot of research has been performed regarding the aspect of inheritance model (Luttikhuizen and Drent, 2008), heritability assessment (Wan et al., 2017) and transcriptome analysis (Yue et al., 2015) of shell color traits in mollusk species. It was reported that shell color may be determined by genetic factors, while environmental factors such as diet, salinity and temperature could have an influence on shell coloration in some species (Heath, 1975; Kobayashi et al., 2004; Liu et al., 2009). For *C. gigas*, Ge et al. (2015b) proposed that the shell background color was controlled by a simple pattern of inheritance, which the golden color was dominant to the white color, and it may have an epistatic effect on foreground pigmentation. Xu et al. (2017) estimated the heritabilities of growth and shell color traits and their genetic correlations in black shell strain of *C. gigas*. The results

* Corresponding author at: Key Laboratory of Mariculture, Ministry of Education, Ocean University of China, 5 Yushan Road, Qingdao 266003, China.
E-mail address: qili66@ouc.edu.cn (Q. Li).

https://doi.org/10.1016/j.aquaculture.2018.04.018
Received 6 December 2017; Received in revised form 8 April 2018; Accepted 10 April 2018
Available online 12 April 2018

suggested that total weight and black shell should be taken as joint objective traits to optimize the selection strategy in selective breeding program. Through comparative transcriptome analysis, some potential shell coloration genes and related molecular mechanisms were revealed in four shell color variants of *C. gigas* (Feng et al., 2015). Despite these progresses, the knowledge of shell color formation and inheritance we have known is still limited for *C. gigas*.

Identifying quantitative trait loci (QTLs) or the genes responsible for shell pigmentation would provide insights into understanding the genetic mechanism of shell coloration. Furthermore, QTLs could be applied in marker-assisted selection (MAS) for *C. gigas* to accelerate the process of selective breeding. The genetic linkage map-based QTL analysis is a powerful and effective approach to detect markers that are significantly associated with desired traits. To date, numbers of QTLs have been identified in > 20 aquatic species (Yue, 2014) and some of them have been successfully applied in MAS commercial breeding programs (Fuji et al., 2007; Moen et al., 2009). Single nucleotide polymorphisms (SNPs) are the most common type of DNA variation in genomes. They have been extensively used in genetic studies due to the advantage of stable and co-dominant inheritance, random distribution in genome, and can be genotyped automatically and high-throughput (Semagn et al., 2006). They are viewed as the ideal DNA markers for constructing a high density genetic map and a powerful tool for dissecting various complex traits (Batra et al., 2014). Specifically, the SNPs derived from the expressed sequence tags (EST-SNPs), as type I markers, are highly valuable in gene mapping and comparative genome analysis because of the ESTs are partial of the expression genes and originated from the conserved transcribed regions (Picoult-Newberg et al., 1999).

In this study, we developed and validated novel SNP markers from EST sequences and constructed an integrated genetic map based on EST-SNP markers with two oyster mapping families. QTL analysis was carried out to detected markers linked to genes associated with shell color and growth traits. The integrated map and identified QTLs would help us understand the molecular mechanism of the important economic traits and provide a basis of MAS for the *C. gigas* in the future.

2. Materials and methods

2.1. Mapping families and parental assignment

Two strains of the Pacific oyster were used to make the mapping panels. In 2010, individuals with white shell color and black shell color were collected from wild populations in Rushan, Shandong Province, China. Selective breeding targeting the traits of pure shell color and fast growth were constructed by successively four-generation family selection from 2010 to 2013 and one-generation mass selection in 2014. In May 2015, the oysters with typical white shell and black shell were selected from the two selective strains, and used to generate two reciprocal-cross F_1 families MF-A (white shell ♀ × black shell ♂) and MF-B (black shell ♀ × white shell ♂) by mating single pair of parents (Fig. 1). The rearing management in larvae, spat and adults stage was implemented according to the procedure described as (Li et al., 2011). When the shell height of the spats reached 2–3 mm after 40 days, they were transported to Rongcheng offshore in Shandong province and cultured on suspended longlines. Adductor muscle of the parents were preserved in 95% ethanol and frozen at −30 °C for DNA analysis.

In 2016, 165 oysters of MF-A and 182 oysters of MF-B were sampled when they were 12-month old. Genomic DNA of the parents and their progeny was extracted from adductor muscle using a modified phenol-chloroform method (Li et al., 2006). For obtaining accurate marker order on a genetic map, it is necessary to exclude the individuals who do not belong to the mapping family. Two informative microsatellite multiplex polymerase chain reaction (PCR) panels (Liu et al., 2017) (Panel 1 and Panel 2, 6 loci) were used for parental assignment in the MF-A and MF-B. The PCR product-size standard-formamide mixture was subjected to capillary electrophoresis on an ABI 3130 Genetic Analyzer (Applied Biosystems) and fragment size was analyzed using GeneMapper v4.0 software (Applied Biosystems).

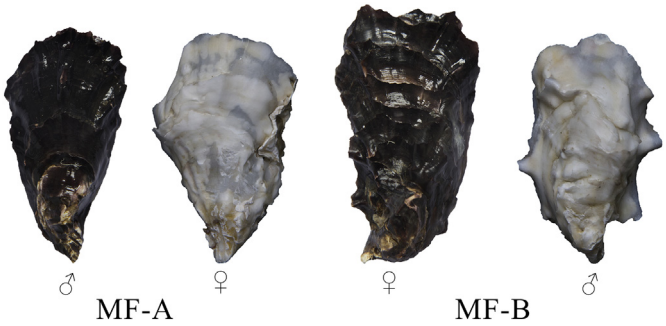

Fig. 1. The parents oysters used for construction the mapping families MF-A and MF-B.

2.2. Growth traits measurement and image capture

For the both mapping populations, their shell height (SH), shell length (SL), shell width (SWi) were measured using a vernier caliper accurate to 0.02 mm. Total weight (TW), shell weight (SWe) and soft-tissue weight (STW) were measured using an electronic balance accurate to 0.01 g.

Shell color can be rapidly analyzed by computerized image analysis techniques, known as computer vision systems (CVS) (Mendoza et al., 2006). The system described by Wan et al. (2017) was applied to precisely quantify standard color of oyster shells. For image acquisition, left shells were placed on a matte black background and illuminated using two 20 W parallel fluorescence lamps. The color temperature of the lamps was 6500 K (D_{65}), a common light source used in food color research. The lamps were assembled 35 cm above the shells and at an angle of 45° to the shell location. A color digital camera (Canon 60D) was fixed on a stand vertically over the shells at a distance of 30 cm to capture images with settings as follows: manual model, ISO 200, lens aperture 5.6, shutter speed 1/160, no zoom, no flash, maximum resolution 5184 × 3456 pixels and images were saved in JPEP format in RGB color coordinates. The camera and lamps were covered with black cloth to avoid the affection of ambient illumination and keep shooting environment as uniform as possible. The camera was connected to a PC with an USB interface. Images can be visualized and acquired directly from the computer through a remote-control software EOS Utility (Canon, USA). All the left shells were pre-treated according to the procedure described by Evans et al. (2009) before taking photos.

2.3. Traits data analysis

Manual cutout was performed precisely using the Adobe Photoshop CS6 (Adobe Systems Inc) to extract shells from the background. Then the RGB color images were convert to lab model to obtain the raw L (lightness), a (redness) and b (yellowness) values from the Histogram Window. The standard color values CIE 1976 L^*, a^* and b^* were computed with the following formulas (Yam and Papadakis, 2004):

$$L^* = \frac{\text{Lightness}}{255} \times 100$$

$$a^* = \frac{240a}{255} - 120$$

$$b^* = \frac{240b}{255} - 120$$

To analysis variation in shell pigmentation coverage (SPC), the total shell area and the dark shell pigmentation in the cutout images were computed using the Image-Pro Plus 6.0 software (Media Cybernetics).

Table 1
Descriptive statistics for the growth traits and shell color parameters of the MF-A and MF-B families.

Traits	MF-A					MF-B				
	Range	Mean ± SD	CV (%)	Skewness	Kurtosis	Range	Mean ± SD	CV (%)	Skewness	Kurtosis
L^*	32.13–75.18	57.68 ± 9.33[a]	16.18	0.02	−0.74	40.34–74.57	63.97 ± 5.74[b]	8.97	−0.87	1.24
a^*	−1.46-1.99	0.03 ± 0.75[a]	7–	0.40	−0.37	−1.04-3.33	0.76 ± 0.87[b]	–	0.43	−0.02
b^*	6.02–20.95	12.74 ± 2.53	19.86	0.11	−0.01	2.80–22.26	12.59 ± 3.22	25.58	−0.14	0.52
SPC	0.01–0.60	0.14 ± 0.12[a]	85.71	1.12	1.32	0.01–0.53	0.17 ± 0.10[b]	58.82	0.95	1.01
SH (mm)	21.26–79.39	54.84 ± 9.27	16.90	−0.15	0.90	30.84–81.19	54.88 ± 8.91	16.24	0.22	0.31
SL (mm)	21.65–53.58	36.88 ± 6.18	16.76	0.00	−0.08	18.80–50.89	36.14 ± 6.39	17.68	−0.11	−0.25
SWi (mm)	11.81–31.10	19.69 ± 3.81[a]	19.35	0.26	−0.10	11.20–29.43	17.95 ± 3.38[b]	33.69	0.28	0.25
TW (g)	6.07–38.08	19.32 ± 7.14	36.96	0.39	−0.32	6.36–41.94	19.08 ± 6.42	33.65	0.54	0.30
SWe (g)	3.78–23.05	11.97 ± 4.43	37.01	0.34	−0.44	3.32–25.00	12.75 ± 4.24	33.25	0.38	0.00
STW (g)	2.07–18.37	7.36 ± 3.22[a]	43.75	0.93	0.86	0.83–16.94	6.37 ± 2.86[b]	44.90	0.87	1.50

CV, variation coefficient; SPC, shell pigmentation coverage; SH, shell height; SL, shell length; SWi, shell width; TW, total weight; SWe, shell weight; STW, soft-tissue weight.
Different letters in the same row means significant difference between MF-A and MF-B at $P < 0.01$.
– Not calculated owing to the exist of minus.

The dark shell pigmentation area was defined as H:255, S:255, I:120 respectively under the HSI color model.

Pearson correlations among the shell color and growth traits were estimated. The differences of phenotype values between the two families were analyzed by *t*-test. Normal tests were conducted by using the kurtosis and skewness coefficients for each measured trait. All these analyses and descriptive statistics were calculated using the SPSS 19.0 (SPSS Inc).

2.4. EST-SNP development and genotyping

Novel EST-SNP development was conducted according to the procedure described as (Zhong et al., 2013). A total of 1794 primer pairs were designed at the flanking sequences of putative SNPs and 576 of them were successfully validated in 32 wild oysters. Information about the 576 SNPs was summarized in Supplementary Table 1.

A total of 1061 EST-SNP markers, containing previously developed 485 EST-SNPs (Zhong et al., 2013; Jin et al., 2014; Zhong et al., 2014a; Zhong et al., 2014b; Wang and Li, 2017) and the new 576 SNP markers were used for polymorphism screening within the two parents and 14 offsprings of each family. These markers were genotyped by using the high-resolution melting (HRM) genotyping technology. The PCR was carried out using the LightCycler®480 real-time PCR system (Roche) with a final volume of 10 μL reaction mix described as Wang and Li (2017): 10 × PCR buffer, 1.5 mM $MgCl_2$, 0.2 mM dNTP mix, 0.2 μM forward and reverse primers, 10 ng template DNA, 0.25 U *Taq* DNA polymerase (Takara) and 5 μM SYTO®9 (Invitrogen). Data were analyzed using the Gene Scanning and Tm Calling programs within LightCycler®480 Software 1.5 (Roche).

2.5. Genetic map construction and QTL analysis

Segregation of each marker was analyzed by chi-square test for the goodness fit of Mendelian ratios. Loci exhibiting significant distorted segregation from Mendelian ratios were also used for the linkage maps construction. JoinMap 4.0 software (Van Ooijen, 2006) was used to construct the sex-average linkage maps for the two families respectively, running the cross-pollinating (CP) population type genotype codes (lm × ll, nn × np, hk × hk). The grouping of linked markers was determined with the followed calculation options: independence logarithm of the odds (LOD) threshold of 6.0, regression mapping algorithm, linkages with a rec. freq. smaller than 0.4 and a LOD larger than 1.00, goodness-of-fit jump threshold for removal of loci 5.00. Recombination rate was transformed to genetic distance in centiMorgans (cM) using the Kosambi mapping function (Kosambi, 2016). Linkage groups were drawn with MapChart2.1 program (Voorrips, 2002). Two approaches (Chakravarti et al., 1991; Fishman et al., 2001) were used for estimating the expected genome length of the genetic maps and the average of the two estimates was calculated as the estimated genome length (Ge). The observed genome length (Go) was the total length of framework map. The genome coverage was determined by Go/Ge.

QTL mapping analysis was conducted by MapQTL 6.0 software using interval mapping algorithm (Van Ooijen, 2009). The LOD score significance thresholds were estimated by 1000 permutation tests at a linkage-group-wide significance level $\alpha < 0.05$ (Doerge and Churchill, 1996). The QTLs are named by the family name (qA or qB) followed by an abbreviation of the trait and the QTL number. Based on the position of homologous flanking markers on the integrated map, comparative QTL analysis was conducted between the two families. If a flanking marker defining a QTL was not linked on the framework map during the merging process, the next most closely linked marker on the integrated map was chosen for representation. When a QTL was mapped to a single marker, the location of this marker was used to represent for the position of the QTL (Zheng et al., 2013). Then the detected QTLs could be annotated by the tightly linked genic SNP markers. The SNP-containing sequences were aligned with the reference genome in the NCBI database using BlastX (Altschul et al., 1990).

For comparative mapping analysis, common SNP markers were identified between the integrated map and the linkage maps reported by Hedgecock et al. (2015). The SNP-containing ESTs were aligned with the draft genome of *C. gigas* (Zhang et al., 2012) for mapping corresponding genome scaffolds.

3. Results

3.1. Phenotypic data analysis

The descriptive statistics of the shell color and growth traits for the two families were summarized in Table 1. There were significant differences between the MF-A and MF-B families in the traits of L^*, a^*, SPC, SWi and STW ($P < 0.01$). For both families, the values of variation coefficients for weight traits (TW, SWe and STW) were larger than morphological characters (SH, SL and SWi), indicating that the difference in weight traits were more significant among the individuals. All the traits except for STW and L^* were followed the normal distribution in the two families ($P < 0.01$). Because of the existence of minus in the a^* dataset, we did not calculate its coefficient of variation.

Pearson correlation analysis showed that all the growth-related traits were significantly correlated in both families, with the maximum correlation coefficients 0.95 in MF-A and 0.93 in MF-B between the total weight and shell weight (Table 2). Conversely, the correlations within shell color related traits and the correlations among growth

Table 2
Correlation coefficients of shell color and growth traits of *C. gigas* (MF-A: below the diagonal; MF-B: above the diagonal).

	*L**	*a**	*b**	SPC	SH	SL	SWi	TW	SWe	STW
*L**		0.08	0.50**	0.24**	0.10	0.06	0.02	0.05	0.06	0.02
*a**	−0.23		0.33**	0.11	0.19*	0.21**	0.10	0.12	0.10	0.13
*b**	0.23**	0.44**		0.10	0.05	0.08	0.04	0.07	0.05	0.07
SPC	0.25**	0.18*	0.15		0.12	0.05	0.06	0.13	−0.05	0.14
SH	−0.01	0.11	0.03	0.13		0.40**	0.40**	0.67**	0.61**	0.59**
SL	−0.07	0.18*	−0.06	0.07	0.35**		0.34**	0.68**	0.68**	0.52**
SWi	−0.02	0.15	0.04	−0.03	0.20*	0.40**		0.59**	0.55**	0.49**
TW	0.00	0.26**	0.14	0.21**	0.58**	0.71**	0.59**		0.93**	0.86**
SWe	−0.02	0.23**	0.10	0.05	0.56**	0.72**	0.57**	0.95**		0.61**
STW	0.03	0.25**	0.17*	0.11	0.52**	0.59**	0.52**	0.91**	0.74**	

SPC, shell pigmentation coverage; SH, shell height; SL, shell length; SWi, shell width; TW, total weight; SWe, shell weight; STW, soft-tissue weight.
* Indicates that the correlation is significant at $P < 0.05$.
** Indicates that the correlation is significant at $P < 0.01$.

related traits and shell color related traits were weak.

3.2. Segregation of SNP markers

Of the 1061 EST-SNP markers, 457 and 394 loci were polymorphic in the two-family parents and their progeny respectively. There were 174 (38.1%) loci in MF-A and 141 (35.8%) loci in MF-B deviated significantly from Mendelian segregation at $P < 0.05$. Most of the departed markers in both families (122 and 106, respectively) were deficient for homozygotes.

3.3. Genetic linkage maps

Based on the SNPs segregation data of the MF-A and MF-B families, two separate sex-average genetic maps were constructed (Table 3). For the genetic map of MF-A (Fig. 2), it was composed of 274 SNP markers which were mapped to 10 linkage groups. The map was 897.71 cM in length, with an average interval of 3.40 cM and a maximum interval of 23.04 cM. The number of SNPs distributed to each linkage group varied from 6 SNPs on LG10 to 54 SNPs on LG1, with an average of 27.4. The longest linkage group was LG2, which was composed of 40 markers with 117.29 cM in length, and the shortest linkage group was LG10, which contained 6 markers with 39.87 cM in length. The average of linkage groups length was 89.78 cM.

For the genetic map of MF-B (Fig. 3), it was composed of 241 SNP markers which were mapped to 10 linkage groups. The map was 805.00 cM in length, with an average interval of 3.48 cM and a maximum interval of 25.85 cM. The number of SNPs distributed to each linkage group varied from 4 SNPs on LG10 to 47 SNPs on LG1, with an average of 24.1. The longest linkage group was LG2, which was composed of 45 markers with 131.09 cM in length, and the shortest linkage group was LG7, which contained 7 markers with 39.87 cM in length. The average length of linkage groups was 80.50 cM.

The estimated genome length of the MF-A and MF-B maps based on the two methods were 976.45 cM and 892.08 cM, respectively. Thus, the framework map coverage was 91.94% for the MF-A and 90.24% for the MF-B.

3.4. Maps integration

According to the anchor markers on the homologous linkages, the two separate linkage maps of MF-A and MF-B were combined into an integrated map (Fig. 4). The integrated map comprised 351 markers and spanned 947.31 cM (*Gof*) in length, with an average interval of 2.78 cM and a maximum interval of 12.85 cM. The number of SNPs distributed to each linkage group varied from 9 SNPs on LG10 to 71 SNPs on LG1, with an average of 35.1. The longest linkage group was LG6, which was composed of 32 markers with 149.23 cM in length, and the shortest linkage group was LG10, which contained 9 markers with 45.26 cM in length. The average length of linkage groups was 94.73 cM.

The expected genome length of the integration map calculated by the two methods was 1002.31 cM and 1024.41 cM, respectively, with an average of 1013.36 cM (*Ge*). Then the genome coverage of the integration map was 93.48% (*Cof*). As the genome size of *C. gigas* was estimated about 557.7 Mb (Zhang et al., 2012), the average recombination rate was ~1.84 cM/Mb across the genome.

3.5. QTL mapping for shell color and growth traits

On the basis of linkage map of MF-A, 11 significant QTLs associated with shell color were detected on LG2, LG4, LG5 and LG10 (Table 4), accounting for a percentage of phenotypic variance explained (PVE) of

Table 3
Summary of the genetic linkage maps of *C. gigas*.

Linkage group	Length(cM)			Marker No.			Average distance(CM)		
	MF-A	MF-B	Integrated map	MF-A	MF-B	Integrated map	MF-A	MF-B	Integrated map
1	100.69	129.90	115.96	54	47	71	1.90	2.82	1.66
2	117.29	131.09	99.82	40	45	60	3.01	2.98	1.69
3	105.28	116.48	97.88	38	31	52	2.85	3.88	1.92
4	89.82	68.22	80.82	34	30	40	2.72	2.35	2.07
5	111.20	70.90	101.91	31	26	38	3.71	2.84	2.75
6	75.72	67.51	139.23	23	26	32	3.44	2.70	4.81
7	85.16	90.59	85.29	22	17	21	4.06	5.66	4.26
8	101.90	39.87	90.59	16	7	17	6.79	6.64	5.66
9	65.93	40.67	80.55	10	8	11	7.33	5.81	8.05
10	44.73	49.78	45.26	6	4	9	8.95	16.59	5.66
Total	897.71	805.00	937.31	274	241	351	3.40	3.48	2.78
Coverage	91.94%	90.24%	93.45%						

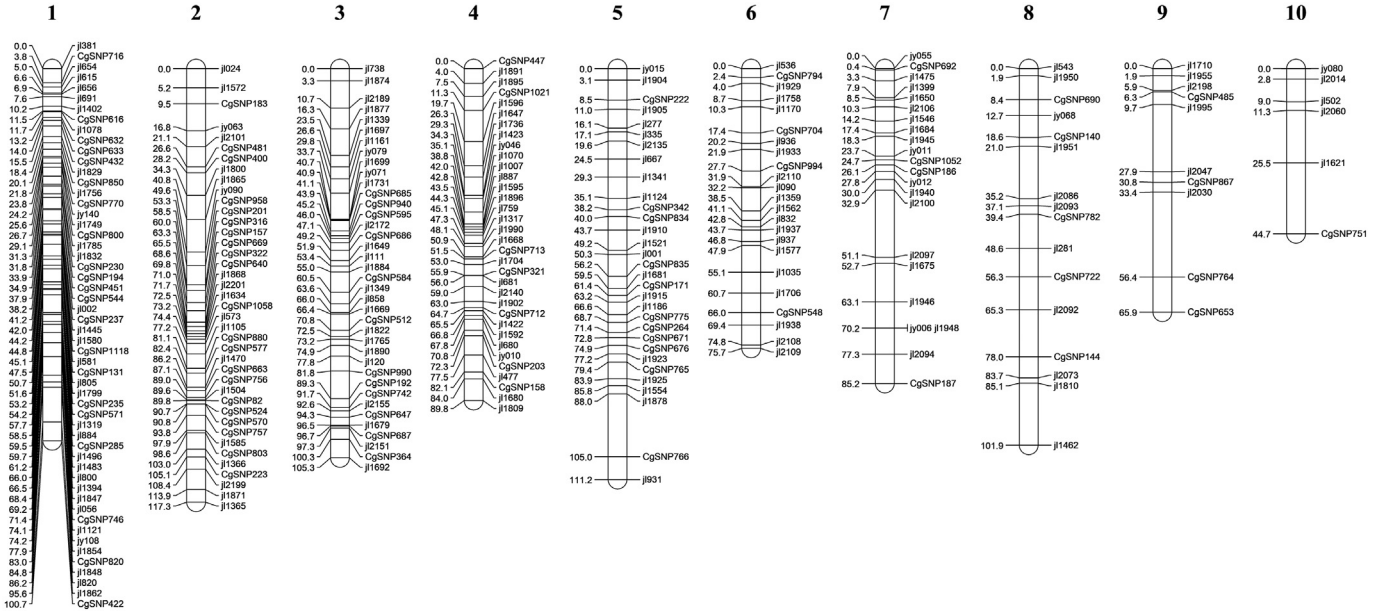

Fig. 2. The linkage map of Pacific oyster (*Crassostrea gigas*) for mapping family A. Marker distances in Kosambi centiMorgans and marker names are indicated on the left and right of each linkage group, respectively.

8.1%–13.8% with an average of 11.76%. The QTLs tended to have pleiotropism: three QTLs mapped to the same region of 71.67 cM on LG2, which located at the SNP marker jl2201, were associated with *L**, *a** and SPC simultaneously, explaining 10.4%, 11.8% and 10.8% phenotypic variation of shell color traits respectively. The QTLs associated with shell color traits of *L** and SPC were mapped to the same two locations: one was located at 71.67 cM on LG2 and one was located at the overlap interval of 33.51–44.73 cM on LG10. Three QTLs for *b** spanned discontinuously from 41.81 to 84.00 cM on LG4. For the growth-related traits, a total of five QTLs were detected on LG3 and LG5, and the average phenotypic variability explained by each QTL was 10.66% (range from 10.4% to 11.0%). Two QTLs for the shell length were at 95.26 and 99.30–102.27 cM on LG3, and one QTL were at 35.13 cM on LG5. The two QTLs (qA-TW 1 and qA-STW 1) for total weight and soft-tissue weight were detected in similar regions of 27.54–32.31 cM and 27.54–30.31 cM on LG5, with the same marker jl1341 in the intervals, showing a PVE of 11.0% and 10.4%, respectively.

For the MF-B, nine significant QTLs detected on LG5 and LG8 (Table 5) were associated with shell color traits, explaining 8.8%–21.7% phenotypic variation. Two of the nine QTLs (qB-*a** 1 and qB-*a** 2) were mapped 0.00–2.29 cM and 28.09–30.09 cM on LG5, and other seven QTLs were spanned discontinuously from 4.01 to 19.87 cM on LG8. Three QTLs controlling the *L**, *b** and SPC were detected at the same region of 4.01 cM on LG8 within the SNP marker jl953, accounting for a percentage of 10.1%, 10.6% and 9.7% PVE respectively. Similarly, another region of overlap interval 15.30–19.87 cM of LG8 were also associated with *L**, *b** and SPC, within the SNP marker jl819, accounting for a high percentage of PVE of 21.7%, 13.1% and 21.0%, respectively. The QTLs associated with shell color traits of *L**and SPC were mapped to the same two locations: one was located nearby 4.01 cM on LG2 and one was located at the interval of 14.30–19.87 cM on LG10. For the growth traits, one QTL associated with SL was found at 37.39 cM on LG4, showing a PVE of 9.0%. Seven QTLs related to TW,

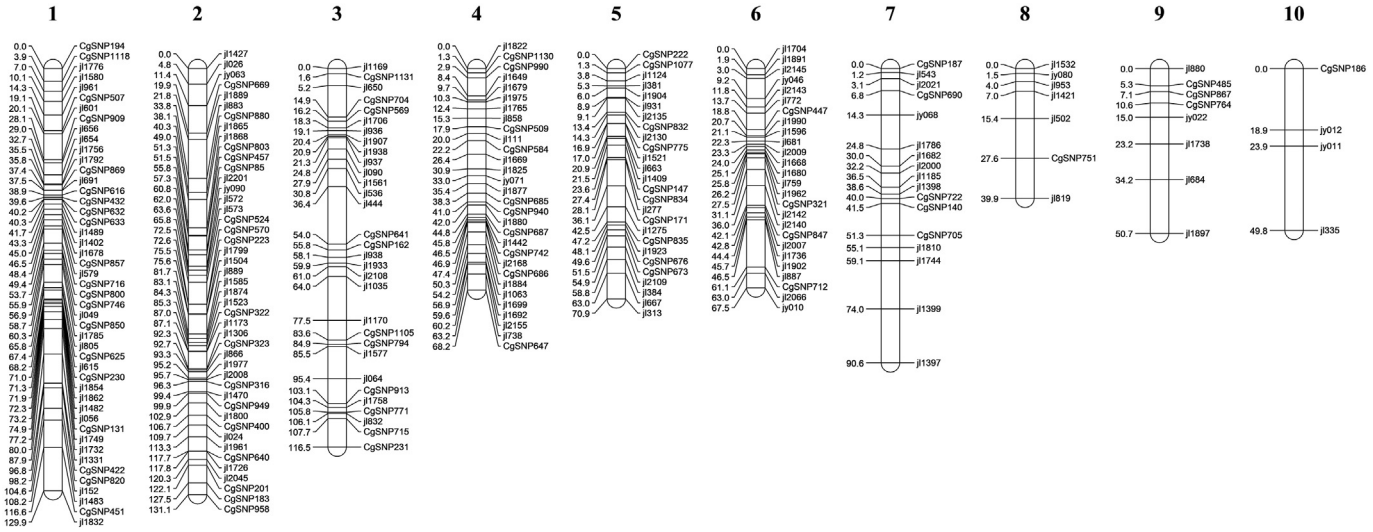

Fig. 3. The linkage map of Pacific oyster (*Crassostrea gigas*) for mapping family B. Marker distances in Kosambi centiMorgans and marker names are indicated on the left and right of each linkage group, respectively.

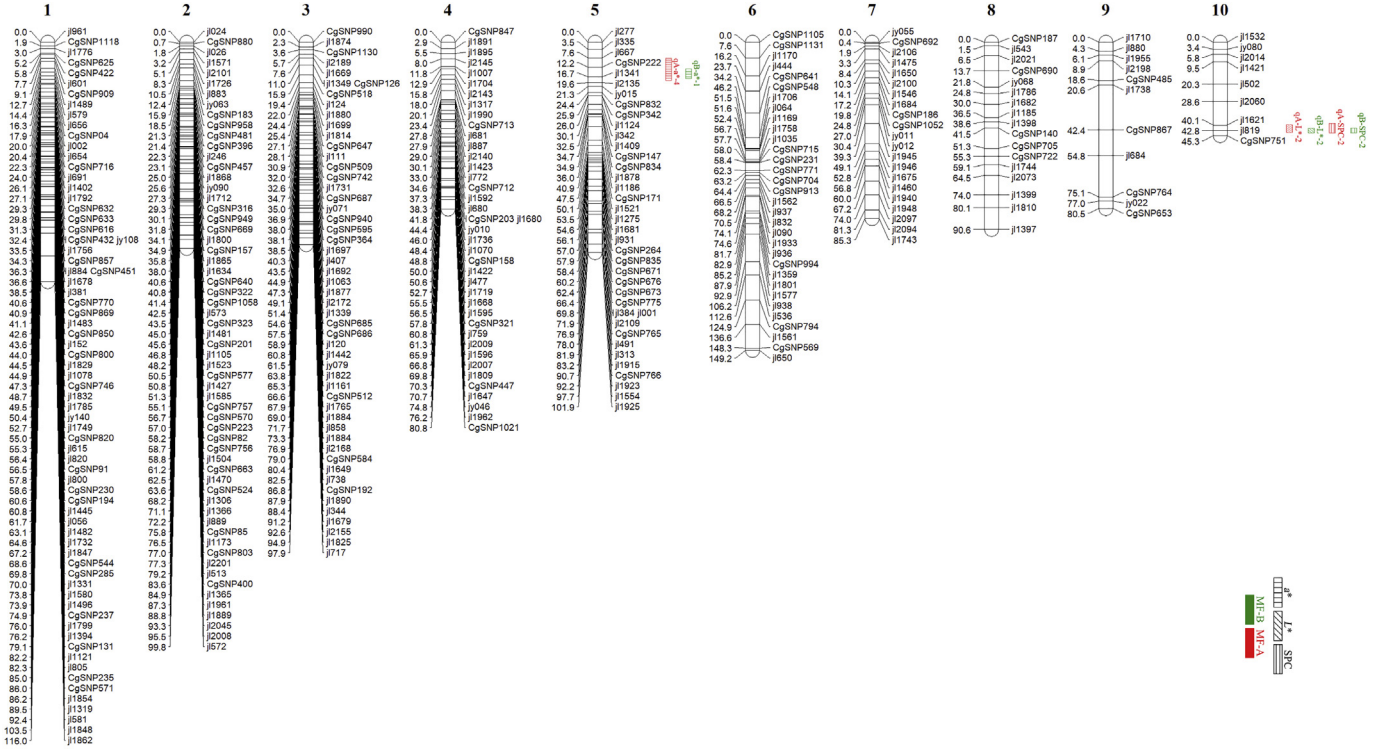

Fig. 4. The integrated linkage map of Pacific oyster (*Crassostrea gigas*) based on mapping family A and mapping family B. Marker distances in Kosambi centiMorgans and marker names are indicated on the left and right of each linkage group, respectively.

SWe and STW tended to colocalize, clustering in a special region of 24.75 to 43.79 cM on LG7, and they accounted for a percentage of PVE of 8.4%–9.4%.

By comparative QTL analysis, three co-occurring significant QTLs were identified on the integrated linkage map (Fig. 4). One *a** shared-QTL (qA-*a** 4/qB-*a** 1) was detected on the linkage group 5, while one *L** shared-QTL (qA-*L** 2/qB-*L** 2) and one SPC shared-QTL (qA-SPC 2/qB-SPC 2) were detected on the linkage group 10 at the same position.

3.6. QTL annotation and comparative mapping analysis

The functional annotation of each detected QTL was summarized in Table 4 and Table 5. The association between several annotated QTLs (like qA-*L** 2 annotated as *C. gigas* furin-like protease 1 and qA-SL 2 annotated as *C. gigas* cilia- and flagella-associated protein 61) and the corresponding traits still remained to be studied further. A few QTLs were annotated as hypothetical protein or their function was unknown or uncharacterized. Notably, the shared-QTL qA-*a** 4 located on the linkage group 5 was highly homologous to *C. gigas* calmodulin-like protein by BlastX search.

Comparative mapping analysis identified two common SNPs (CgSNP223/502-G307268A and jl1562/1492-A151764C) between the integrated map and the linkage maps constructed by Hedgecock et al. (2015). All of the 351 SNPs on the integrated map were mapped to 267 scaffolds of the draft genome (Supplementary Table 2), with 207 containing one SNP and 60 containing two or more SNPs (Supplementary Table 3). Furthermore, 34 (56.67%) of the 60 scaffolds with two or more SNPs were mapped to two or three linkage groups (Supplementary Table 4), implying that the genome scaffolds of *C. gigas* may be incorrectly assembled.

4. Discussion

High heterozygosity is revealed by whole-genome sequencing in marine invertebrates (Sodergren et al., 2006; Small et al., 2007). *C. gigas* is a typical aquatic species with high levels of polymorphism, which means that abundant SNPs are present in the genome. It was estimated that the average SNP frequency was one per 60 bp in coding regions and one per 40 bp in non-coding regions (Sauvage et al., 2007). The level of polymorphism revealed by complete genome sequence of *C. gigas* was 2.3% (Zhang et al., 2012), higher than that in *Caenorhabditis elegans* (0.06%; Hillier et al., 2008) and human (0.09%; Venter et al., 2001). The abundant variations would provide valuable resources for oyster genetic improvement in breeding practices.

Several approaches have been developed for SNP genotyping, such as single-strand conformation polymorphism (SSCP) analysis (Hayashi, 1991), denaturing gradient gel electrophoresis (DGGE) (Lerman and Silverstein, 1987), denaturing high-performance liquid chromatography (DHPLC) (Xiao and Oefner, 2001) and direct sequencing (Shattuck-Eidens et al., 1990). These mutation scanning methods require separation steps and increase the risk of contamination as the PCR products are exposed to the environment (Reed and Wittwer, 2004). Particularly, due to the rapid advance in next-generation sequencing technologies, they have been widely employed to genotype SNPs (Andrews et al., 2016). Despite the advantages in quantity, the relative high cost cannot be ignored, especially in the cases of large genomes and sequencing with high-coverage to avoid high SNP calling error rate (Qi et al., 2017). Those methods based on reduced genome sequencing, like GBS and RAD-seq, digest the genome DNA with one or two enzymes and then sequencing the selected restriction fragments with suitable length, which makes it difficult to share and transfer the data among different laboratories within different oyster populations (Elshire et al., 2011; Peterson et al., 2012). Furthermore, huge data would be obtained after sequencing using the NGS technologies, intensive and complex subsequent bioinformatics analysis steps are still needed for acquiring useful information.

Alternatively, HRM is an economic, efficient and closed-tube SNP genotyping method. It only requires a saturation dye and a high-resolution melting instrument compare to conventional PCR to detect the differences in the sequences even with only single-base variants. After

Table 4
Summary of quantitative trait loci for shell color and growth traits in mapping family A.

Trait	QTL	Linkage group	Interval (cM)	Peak position (cM)	Nearest marker	LOD threshold	PVE (%)	Annotation
L^*	qA-L^* 1	LG2	71.67	71.67	jl2201	3.4	10.4	*Crassostrea gigas* hypothetical protein (LOC105326360), transcript variant ×3, mRNA
	qA-L^* 2	LG10	33.51–44.73	42.51	CgSNP751	2.5	8.1	PREDICTED: *Crassostrea gigas* furin-like protease 1 (LOC105337074), mRNA
a^*	qA-a^* 1	LG2	71.67	71.67	jl2201	3.3	11.8	*Crassostrea gigas* hypothetical protein (LOC105326360), transcript variant ×3, mRNA
	qA-a^* 2	LG2	88.06–94.80	90.76	CgSNP570	3.3	9.6	PREDICTED: *Crassostrea gigas* uncharacterized LOC105323307 (LOC105323307), mRNA
	qA-a^* 3	LG5	11.03–16.12	13.03	jl1905	3.4	11.6	PREDICTED: *Crassostrea gigas* gamma-tubulin complex component 4 (LOC105330131), mRNA
	qA-a^* 4	LG5	19.10–25.54	24.54	jl667	3.4	11.0	PREDICTED: *Crassostrea gigas* calmodulin-like (LOC105344225), mRNA
b^*	qA-b^* 1	LG4	41.81–42.03	42.03	jl1007	3.4	10.0	PREDICTED: *Crassostrea gigas* double-stranded RNA-specific editase 1-like (LOC105329897), transcript variant ×3, mRNA
	qA-b^* 2	LG4	64.69	64.69	CgSNP712	3.4	10.8	PREDICTED: *Crassostrea gigas* NAD(P) transhydrogenase, mitochondrial (LOC105343392), mRNA
	qA-b^* 3	LG4	83.14–84.00	84.00	jl1680	3.4	10.5	PREDICTED: *Crassostrea gigas* tRNA wybutosine-synthesizing protein 2 homolog (LOC105332610), transcript variant ×4, mRNA
SPC	qA-SPC 1	LG2	71.67	71.67	jl2201	3.9	13.8	*Crassostrea gigas* hypothetical protein (LOC105326360), transcript variant ×3, mRNA
	qA-SPC 2	LG10	26.51–44.73	38.51	CgSNP751	2.7	10.8	PREDICTED: *Crassostrea gigas* furin-like protease 1 (LOC105337074), mRNA
SL	qA-SL 1	LG3	95.26	95.26	CgSNP647	3.5	10.6	PREDICTED: *Crassostrea gigas* uncharacterized LOC105342035 (LOC105342035), partial mRNA
	qA-SL 2	LG3	99.30–102.27	100.27	CgSNP364	3.5	10.7	PREDICTED: *Crassostrea gigas* cilia- and flagella-associated protein 61 (LOC105320109), transcript variant ×2, mRNA
	qA-SL 3	LG5	35.13	35.13	jl1124	3.4	10.6	PREDICTED: *Crassostrea gigas* protocadherin-like wing polarity protein stan (LOC105330278), transcript variant ×2, mRNA
TW	qA-TW 1	LG5	27.54–32.31	29.31	jl1341	3.4	11.0	PREDICTED: *Crassostrea gigas* kidney mitochondrial carrier protein 1 (LOC105333794), mRNA
STW	qA-STW 1	LG5	27.54–30.31	28.54	jl1341	3.6	10.4	PREDICTED: *Crassostrea gigas* kidney mitochondrial carrier protein 1 (LOC105333794), mRNA

PVE, percentage of phenotypic variance explained; SPC, shell pigmentation coverage; SL, shell length; TW, total weight; STW, soft-tissue weight.

PCR amplification, melting curves are generated by monitoring the decreasing fluorescence of saturation dye intercalated in the double-stranded DNA. Then the heterozygotes and homozygotes can be identified by a difference of melting curve shapes and a shift in melting temperature (T_m) (Wittwer et al., 2003; Reed et al., 2007). Combining with the HRM genotyping technology, the EST-derived SNPs have been widely developed and used in animal and plant genetic studies (Distefano et al., 2013; Dong et al., 2016; Wang et al., 2015; Zhan et al., 2016). The EST-derived SNPs could be transferred and amplified well in different populations and even related species in the *Crassostrea* genus (Zhong et al., 2014b), the collinearity and synteny could be analyzed using the anchor SNP markers in comparative mapping analysis. As the EST-SNPs were genic, their location information in the genome could be identified by the specific primers, which would be highly valuable in assisting in genome assembly and identification of functional genes related with commercially and ecologically important traits.

Although initiated later in linkage mapping than other agricultural animals, great progress has been made for aquatic species over the past two decades (Kocher and Kole, 2008). For *C. gigas*, several linkage maps were published mainly using amplified fragment-length polymorphism (AFLP), microsatellite or a small number of SNP markers (Hubert and Hedgecock, 2004; Li and Guo, 2004; Hubert et al., 2009; Sauvage et al., 2010; Plough and Hedgecock, 2011; Guo et al., 2012; Zhong et al., 2014a). The defect of low-density and coverage limited their potential application in QTL fine mapping. More recently, the GoldenGate microarray and GBS SNP genotyping platforms were used for constructing high density second-generation linkage maps (Hedgecock et al., 2015; Wang et al., 2016), which were not available for every laboratory in consideration of the relative high cost. In the present study, two mapping populations were established by reciprocal cross between the black shell and white shell oysters for constructing two separate linkage maps, using EST-SNP markers combined with the HRM genotyping technology, and then merging them into an integrated map. The density and coverage of the integrated map was improved compared to the two separate maps, with an average distance of 2.78 cM between markers. Using two or more reference populations, more markers would be informative in at least one of the populations and mapped into the linkage maps. This mapping strategy has been successfully applied in some aquatic species, such as the Barramundi *Lates calcarifer* (Wang et al., 2007) and grass carp *Ctenopharyngodon idella*. (Xia et al., 2010). The integrated linkage map spanned 947.31 cM in length and a total of 351 EST-SNPs were assigned to 10 LGs, which were in accordance with the haploid number of chromosomes (2n = 20) in the species. The discordance between the linkage groups number and the haploid chromosomes number was found in previously published genetic maps of *C. gigas* (Hubert and Hedgecock, 2004; Li and Guo, 2004; Guo et al., 2012). The low density and uneven distribution of markers may lead to the result. More markers that could fill the gaps between the separate linkage groups should be added to integrate them into one linkage group. Large gaps were still observed in the present map, indicating that high recombination rates or lacing of sufficient polymorphism markers may be present in the regions. A higher density map could be obtained by adding more new SNPs and other markers in the future.

The phenomenon that significant segregation distortion from Mendelian ratios was common in linkage mapping studies and its level varied among different type markers and species (Shi et al., 2014). Of the 351 mapped markers on the present integrated map, 118 (33.62%) were departed from Mendelian segregation, higher than that of AFLP and microsatellites markers in previous studies of *C. gigas* (Li and Guo, 2004; Guo et al., 2012) and other marine mollusks species (Yu and Guo, 2003; Li et al., 2005). Several reasons may lead to the deviation from Mendelian expectations, such as zygotic selection, non-random segregation during meiosis and duplicated genes (Lyttle, 1991; Pardo-Manuel de Villena and Sapienza, 2001; Gut and Lathrop, 2004). It has been proved that a high genetic load of deleterious recessive mutations is responsible for no-Mendelian inheritance of markers in *C. gigas*

Table 5
Summary of quantitative trait loci for shell color and growth traits in mapping family B.

Trait	QTL	Linkage group	Interval (cM)	Peak position (cM)	Nearest marker	LOD threshold	PVE (%)	Annotation
*L**	qB-*L** 1	LG8	4.01	4.01	jl953	2.8	10.1	Unknown
	qB-*L** 2	LG8	14.30–19.87	19.87	jl819	2.8	21.7	PREDICTED: *Crassostrea gigas* uncharacterized LOC105346399 (LOC105346399), transcript variant ×3, mRNA
*a**	qB-*a** 1	LG5	0.00–2.29	1.29	CgSNP1077	3.3	11.6	PREDICTED: *Crassostrea gigas* uncharacterized LOC105341982 (LOC105341982), mRNA
	qB-*a** 2	LG5	28.09–30.09	28.09	jl277	3.3	9.0	PREDICTED: *Crassostrea gigas* succinate–CoA ligase [ADP/GDP-forming] subunit alpha, mitochondrial (LOC105319941), transcript variant ×4, mRNA
*b**	qB-*b** 1	LG8	4.01	4.01	jl953	2.8	10.6	Unknown
	qB-*b** 2	LG8	7.01–9.03	7.03	jl1421	2.8	8.8	PREDICTED: *Crassostrea gigas* cell wall protein DAN4 (LOC105332709), transcript variant ×2, mRNA
	qB-*b** 3	LG8	15.30–19.87	19.87	jl819	2.8	13.1	PREDICTED: *Crassostrea gigas* uncharacterized LOC105346399 (LOC105346399), transcript variant ×3, mRNA
SPC	qB-SPC 1	LG8	3.37–4.01	4.01	jl953	2.8	9.7	Unknown
	qB-SPC 2	LG8	14.30–19.87	19.87	jl819	2.8	21.0	PREDICTED: *Crassostrea gigas* uncharacterized LOC105346399 (LOC105346399), transcript variant ×3, mRNA
SL	qB-SL 1	LG4	37.39	37.39	CgSNP685	3.5	9.0	PREDICTED: *Crassostrea gigas* stabilizer of axonemal microtubules 2 (LOC105344414), transcript variant ×3, mRNA
TW	qB-TW 1	LG7	24.75–30.98	29.75	jl1682	3.0	9.4	PREDICTED: *Crassostrea gigas* tRNA wybutosine-synthesizing protein 2 homolog (LOC105332610), transcript variant ×4, mRNA
	qB-TW 2	LG7	34.20–37.52	35.20	jl1185	3.0	9.1	PREDICTED: *Crassostrea gigas* uncharacterized LOC105319128 (LOC105319128), mRNA
	qB-TW 3	LG7	39.55–43.49	41.49	CgSNP140	3.0	8.9	PREDICTED: *Crassostrea gigas* uncharacterized LOC105336641 (LOC105336641), ncRNA
SWe	qB-SWe 1	LG7	27.75–30.98	30.98	jl1682	3.1	9.1	PREDICTED: *Crassostrea gigas* tRNA wybutosine-synthesizing protein 2 homolog (LOC105332610), transcript variant ×4, mRNA
	qB-SWe 2	LG7	34.20–36.20	34.20	jl1185	3.1	8.5	PREDICTED: *Crassostrea gigas* uncharacterized LOC105319128 (LOC105319128), mRNA
STW	qB-STW 1	LG7	24.75–29.98	27.75	jl1682	3.1	8.6	PREDICTED: *Crassostrea gigas* tRNA wybutosine-synthesizing protein 2 homolog (LOC105332610), transcript variant ×4, mRNA
	qB-STW 2	LG7	41.03–42.49	41.49	CgSNP140	3.1	8.4	PREDICTED: *Crassostrea gigas* uncharacterized LOC105336641 (LOC105336641), ncRNA

PVE, percentage of phenotypic variance explained; SPC, shell pigmentation coverage; SL, shell length; TW, total weight; SWe, shell weight; STW, soft-tissue weight.

(Launey and Hedgecock, 2001). Hubert and Hedgecock (2004) constructed consensus linkage maps for the *C. gigas* by genotyping 11-day-old larvae and the distorted segregation ratios was effectively reduced in the mapping families, indicating that a high genetic load of deleterious recessive mutations leading to strong zygotic selection during the larval stage was a cause of segregation distortion. There have been several studies demonstrated that adding distorted markers moderately would benefit linkage map construction (Fishman et al., 2001; Lanteri et al., 2006). Here, the distorted markers were utilized for constructing the genetic maps, as they were useful in mapping the deleterious recessive genes (Li and Guo, 2004; Guo et al., 2012).

QTL mapping analyses have been conducted mainly for the traits of growth and disease resistance (Yu and Guo, 2006; Sauvage et al., 2010; Guo et al., 2012; Wang et al., 2016), and seldom for inbreeding depression (Plough and Hedgecock, 2011), glycogen and shell pigmentation in oysters (Zhong et al., 2014a; Ge et al., 2015a). Color as an economic important trait, a few of color-related QTLs have been detected in aquaculture species (Qin et al., 2007; Boulding et al., 2008; Baranski et al., 2010; Petersen et al., 2012). Ge et al. (2014) identified a SCAR marker that linked to a major gene/QTL controlling the shell pigmentation for *C. gigas* and mapped it onto a reference genetic map. Seven QTLs associated with shell nacre color with a percentage of PVE of 19.7% to 22.8%, were detected in triangle sail mussel *Hyriopsis cumingii* (Bai et al., 2016). Of the seven QTLs, five QTLs were clustered in a special region on one linkage group. A similar result was found in the present two mapping families, QTLs for both shell color and growth traits showed a tendency to concentrate within narrow intervals, indicating that the genes controlling the shell color and growth traits maybe located in these regions. In the present study, we found the phenomenon of pleiotropism, that is, a same region (like 71.67 cM on LG2 of the MF-A and 27.75 cM–30.98 cM on LG7 of the MF-B) on the linkage group could be associated with diverse traits simultaneously. This conformed to the significant correlations detected among shell color and growth traits. However, the correlations among shell color and grow traits were relative low, implying that the indirect selection for shell color through growth is not feasible and we should take them as joint target traits in selective breeding practices. This conclusion has also been drawn in other studies (Wan et al., 2017; Xu et al., 2017). As markers may not segregate in two specific parents, some important linkage information would lost in QTLs mapping, and therefore the ablity to detect QTLs in a single population is often limited. Conducting QTL mapping analysis with multipe populations would improve the efficiency and accuracy of detecting QTLs and provide insight into their funcational alleleic variation and distribution (Marcel et al., 2007; Wang et al., 2008). In this study, most of the detected QTLs (81.25% for MF-A and 82.35% for MF-B) were family-specific. Three shared-QTLs for shell color traits but no shared-QTL for growth traits were detected within the two mapping families. This may be because growth traits are controlled by a number of genes with small effects, which is consistent with the result of the relative low phenotypic variances explained by the QTLs.

The shared QTL of qA-*a** 4 for shell color traits was annotated as the *C. gigas* calmodulin-like protein, which have been identified to be involved in shell formation in bivalve species (Yan et al., 2007; Fang et al., 2008; Shi et al., 2013). In *P. yessoensis*, it is suggested that the calmodulin-like protein gene is also probably related to melanin biosynthesis of the shell (Sun et al., 2015). In future, more studies should be conducted on the gene to help us understand the relationship between biomineralization and pigmentation in molluscs.

In conclusion, we provided an extensive and valuable resource of EST-SNP markers for *C. gigas*. An integrated linkage map was constructed based on two F_1 families with EST-SNPs, which is potential to play a role in QTL fine mapping and comparative mapping analysis. The QTLs detected in the present study would facilitate in identifying genes controlling shell color and growth traits and provide a basis of MAS for *C. gigas*.

Supplementary data to this article can be found online at https://doi.org/10.1016/j.aquaculture.2018.04.018.

Acknowledgements

This study was supported by grants from National Natural Science Foundation of China (31772843), Taishan Scholars Seed Project of Shandong, and Shandong Province (2016ZDJS06A06).

References

Alfnes, F., Guttormsen, A.G., Steine, G., Kolstad, K., 2006. Consumers' willingness to pay for the color of salmon: a choice experiment with real economic incentives. Am. J. Agric. Econ. 88, 1050–1061.
Altschul, S.F., Gish, W., Miller, W., Myers, E.W., Lipman, D.J., 1990. Basic local alignment search tool. J. Mol. Biol. 215, 403–410.
Andrews, K.R., Good, J.M., Miller, M.R., Luikart, G., Hohenlohe, P.A., 2016. Harnessing the power of RADseq for ecological and evolutionary genomics. Nat. Rev. Genet. 17, 81–92.
Bai, Z.-Y., Han, X.-K., Liu, X.-J., Li, Q.-Q., Li, J.-L., 2016. Construction of a high-density genetic map and QTL mapping for pearl quality-related traits in *Hyriopsis cumingii*. Sci.Rep. 6.
Baranski, M., Moen, T., Våge, D.I., 2010. Mapping of quantitative trait loci for flesh colour and growth traits in Atlantic salmon (*Salmo salar*). Genet. Sel. Evol. 42, 17.
Batra, J., Srinivasan, S., Clements, J., 2014. Single nucleotide polymorphisms (SNPs). In: Yousef, G.M., Jothy, S. (Eds.), Molecular Testing in Cancer. Springer New York, New York, NY, pp. 55–80.
Boulding, E., Culling, M., Glebe, B., Berg, P., Lien, S., Moen, T., 2008. Conservation genomics of Atlantic salmon: SNPs associated with QTLs for adaptive traits in parr from four trans-Atlantic backcrosses. Heredity 101, 381–389.
Brake, J., Evans, F., Langdon, C., 2004. Evidence for genetic control of pigmentation of shell and mantle edge in selected families of Pacific oysters, *Crassostrea gigas*. Aquaculture 229, 89–98.
Chakravarti, A., Lasher, L.K., Reefer, J.E., 1991. A maximum likelihood method for estimating genome length using genetic linkage data. Genetics 128, 175–182.
Clydesdale, F.M., 1993. Color as a factor in food choice. Crit. Rev. Food Sci. 33, 83–101.
Comfort, A., 1951. The pigmentation of molluscan shells. Biol. Rec. 26, 285–301.
de Villena, F.P.-M., Sapienza, C., 2001. Nonrandom segregation during meiosis: the unfairness of females. Mann. Genome 12, 331–339.
Distefano, G., La Malfa, S., Gentile, A., Wu, S.-B., 2013. EST-SNP genotyping of citrus species using high-resolution melting curve analysis. Tree Genet. Genomes 9, 1271–1281.
Doerge, R.W., Churchill, G.A., 1996. Permutation tests for multiple loci affecting a quantitative character. Genetics 142, 285–294.
Dong, Y., Li, Q., Zhong, X., Kong, L., 2016. Development of gene-derived SNP markers and their application for the assessment of genetic diversity in wild and cultured populations in sea cucumber, *Apostichopus japonicus*. J. World Aquacult. Soc. 47, 873–888.
Elshire, R.J., Glaubitz, J.C., Sun, Q., Poland, J.A., Kawamoto, K., Buckler, E.S., Mitchell, S.E., 2011. A robust, simple genotyping-by-sequencing (GBS) approach for high diversity species. PLoS One 6, e19379.
Evans, S., Camara, M.D., Langdon, C.J., 2009. Heritability of shell pigmentation in the Pacific oyster, *Crassostrea gigas*. Aquaculture 286, 211–216.
Fang, Z., Yan, Z., Li, S., Wang, Q., Cao, W., Xu, G., Xiong, X., Xie, L., Zhang, R., 2008. Localization of calmodulin and calmodulin-like protein and their functions in biomineralization in *P. fucata*. Prog. Nat. Sci. 18, 405–412.
FAO, 2014. The State of World Fisheries and Aquaculture. Food and Agriculture Organization of the United Nations, Rome, Italy.
Feng, D., Li, Q., Yu, H., Zhao, X., Kong, L., 2015. Comparative transcriptome analysis of the Pacific Oyster *Crassostrea gigas* characterized by shell colors: identification of genetic bases potentially involved in pigmentation. PLoS One 10, e0145257.
Fishman, L., Kelly, A.J., Morgan, E., Willis, J.H., 2001. A genetic map in the *Mimulus guttatus* species complex reveals transmission ratio distortion due to heterospecific interactions. Genetics 159, 1701–1716.
Fuji, K., Hasegawa, O., Honda, K., Kumasaka, K., Sakamoto, T., Okamoto, N., 2007. Marker-assisted breeding of a lymphocystis disease-resistant Japanese flounder (*Paralichthys olivaceus*). Aquaculture 272, 291–295.
Ge, J., Li, Q., Yu, H., Kong, L., 2014. Identification and mapping of a SCAR marker linked to a locus involved in shell pigmentation of the Pacific oyster (*Crassostrea gigas*). Aquaculture 434, 249–253.
Ge, J., Li, Q., Yu, H., Kong, L., 2015a. Identification of single-locus PCR-based markers linked to shell background color in the Pacific oyster (*Crassostrea gigas*). Mar. Biotechnol. 17, 655–662.
Ge, J., Li, Q., Yu, H., Kong, L., 2015b. Mendelian inheritance of golden shell color in the Pacific oyster *Crassostrea gigas*. Aquaculture 441, 21–24.
Guo, X., Li, Q., Wang, Q.Z., Kong, L.F., 2012. Genetic mapping and QTL analysis of growth-related traits in the Pacific oyster. Mar. Biotechnol. 14, 218–226.
Gut, I.G., Lathrop, G.M., 2004. Duplicating SNPs. Nat. Genet. 36, 789–790.
Hayashi, K., 1991. PCR-SSCP: a simple and sensitive method for detection of mutations. Gene PCR Methods Appl. 1, 34–38.
Heath, D., 1975. Colour, sunlight and internal temperatures in the land-snail *Cepaea nemoralis* (L.). Oecologia 19, 29–38.

Hedgecock, D., Shin, G., Gracey, A.Y., Van Den Berg, D., Samanta, M.P., 2015. Second-generation linkage maps for the pacific oyster *Crassostrea gigas* reveal errors in assembly of genome scaffolds. Genes Genom. Genet. 5, 2007–2019.
Hillier, L.W., Marth, G.T., Quinlan, A.R., Dooling, D., Fewell, G., Barnett, D., Fox, P., Glasscock, J.I., Hickenbotham, M., Huang, W., 2008. Whole-genome sequencing and variant discovery in *C. elegans*. Nat. Methods 5, 183–188.
Hubert, S., Hedgecock, D., 2004. Linkage maps of microsatellite DNA markers for the Pacific oyster *Crassostrea gigas*. Genetics 168, 351–362.
Hubert, S., Cognard, E., Hedgecock, D., 2009. Centromere mapping in triploid families of the Pacific oyster *Crassostrea gigas* (Thunberg). Aquaculture 288, 172–183.
Jin, Y.-L., Kong, L.-F., Yu, H., Li, Q., 2014. Development, inheritance and evaluation of 55 novel single nucleotide polymorphism markers for parentage assignment in the Pacific oyster (*Crassostrea gigas*). Genes Genom. 36, 129–141.
Kang, J.-H., Kang, H.-S., Lee, J.-M., An, C.-M., Kim, S.-Y., Lee, Y.-M., Kim, J.-J., 2013. Characterizations of shell and mantle edge pigmentation of a Pacific oyster, *Crassostrea gigas*, in Korean Peninsula. Asian Austral. J. Anim. 26, 1659.
Kobayashi, T., Kawahara, I., Hasekura, O., Kijima, A., 2004. Genetic control of bluish shell color variation in the Pacific abalone, *Haliotis discus hannai*. J. Shellfish Res. 23, 1153–1157.
Kocher, T.D., Kole, C., 2008. Genome Mapping and Genomics in Fishes and Aquatic Animals. Springer, New York.
Kosambi, D.D., 2016. The estimation of map distances from recombination values. Ann. Eugenics 12, 172–175.
Lanteri, S., Acquadro, A., Comino, C., Mauro, R., Mauromicale, G., Portis, E., 2006. A first linkage map of globe artichoke (*Cynara cardunculus var. scolymus* L.) based on AFLP, S-SAP, M-AFLP and microsatellite markers. Theor. Appl. Genet. 112, 1532–1542.
Launey, S., Hedgecock, D., 2001. High genetic load in the Pacific oyster *Crassostrea gigas*. Genetics 159, 255–265.
Lerman, L.S., Silverstein, K., 1987. Computational simulation of DNA melting and its application to denaturing gradient gel electrophoresis. Methods Enzymol. 155, 482–501.
Li, L., Guo, X., 2004. AFLP-based genetic linkage maps of the Pacific oyster *Crassostrea gigas* Thunberg. Mar. Biotechnol. 6, 26–36.
Li, L., Xiang, J., Liu, X., Zhang, Y., Dong, B., Zhang, X., 2005. Construction of AFLP-based genetic linkage map for Zhikong scallop, *Chlamys farreri* Jones et Preston and mapping of sex-linked markers. Aquaculture 245, 63–73.
Li, Q., Yu, H., Yu, R., 2006. Genetic variability assessed by microsatellites in cultured populations of the Pacific oyster (*Crassostrea gigas*) in China. Aquaculture 259, 95–102.
Li, Q., Wang, Q., Liu, S., Kong, L., 2011. Selection response and realized heritability for growth in three stocks of the Pacific oyster *Crassostrea gigas*. Fish. Sci. 77, 643–648.
Liu, X., Wu, F., Zhao, H., Zhang, G., Guo, X., 2009. A novel shell color variant of the Pacific abalone *Haliotis discus hannai* Ino subject to genetic control and dietary influence. J. Shellfish Res. 28, 419–424.
Liu, T., Li, Q., Song, J., Yu, H., 2017. Development of genomic microsatellite multiplex PCR using dye-labeled universal primer and its validation in pedigree analysis of Pacific oyster (*Crassostrea gigas*). J. Ocean U. China 16, 151–160.
Luttikhuizen, P., Drent, J., 2008. Inheritance of predominantly hidden shell colours in *Macoma balthica* (L.) (Bivalvia: Tellinidae). J. Molluscan Stud. 74, 363–371.
Lyttle, T.W., 1991. Segregation distorters. Annu. Rev. Genet. 25, 511–581.
Mann, R., 1991. The decline of the Virginia oyster fishery in Chesapeake Bay: considerations for introduction of a non-endemic species, *Crassostrea gigas* (Thunberg, 1793). J. Shellfish Res. 10, 379–388.
Marcel, T.C., Varshney, R.K., Barbieri, M., Jafary, H., Kock, M.J.D.D., Graner, A., Niks, R.E., 2007. A high-density consensus map of barley to compare the distribution of QTLs for partial resistance to *Puccinia hordei* and of defence gene homologues. Theor. Appl. Genet. 114, 487–500.
Mendoza, F., Dejmek, P., Aguilera, J.M., 2006. Calibrated color measurements of agricultural foods using image analysis. Postharvest Biol. Technol. 41, 285–295.
Moen, T., Baranski, M., Sonesson, A.K., Kjøglum, S., 2009. Confirmation and fine-mapping of a major QTL for resistance to infectious pancreatic necrosis in Atlantic salmon (*Salmo salar*): population-level associations between markers and trait. BMC Genomics 10, 368.
Nell, J.A., 2001. The history of oyster farming in Australia. Mar. Fish. Rev. 63, 14–25.
Orensanz, J.M.L., Schwindt, E., Pastorino, G., Bortolus, A., Casas, G., Darrigran, G., Elías, R., Gappa, J.J.L., Obenat, S., Pascual, M., 2002. No longer the pristine confines of the world ocean: a survey of exotic marine species in the southwestern Atlantic. Biol. Invasions 4, 115–143.
Petersen, J.L., Baerwald, M.R., Ibarra, A.M., May, B., 2012. A first-generation linkage map of the Pacific lion-paw scallop (*Nodipecten subnodosus*): initial evidence of QTL for size traits and markers linked to orange shell color. Aquaculture 350, 200–209.
Peterson, B.K., Weber, J.N., Kay, E.H., Fisher, H.S., Hoekstra, H.E., 2012. Double digest RADseq: an inexpensive method for de novo SNP discovery and genotyping in model and non-model species. PLoS One 7, e37135.
Picoult-Newberg, L., Ideker, T.E., Pohl, M.G., Taylor, S.L., Donaldson, M.A., Nickerson, D.A., Boyce-Jacino, M., 1999. Mining SNPs from EST databases. Genome Res. 9, 167–174.
Plough, L.V., Hedgecock, D., 2011. Quantitative trait locus analysis of stage-specific inbreeding depression in the Pacific oyster *Crassostrea gigas*. Genetics 189, 1473–1486.
Qi, H., Song, K., Li, C., Wang, W., Li, B., Li, L., Zhang, G., 2017. Construction and evaluation of a high-density SNP array for the Pacific oyster (*Crassostrea gigas*). PLoS One 12, e0174007.
Qin, Y., Liu, X., Zhang, H., Zhang, G., Guo, X., 2007. Identification and mapping of AFLP markers linked to shell color in bay scallop, *Argopecten irradians irradians* (Lamarck, 1819). Mar. Biotechnol. 9, 66–73.
Reed, G.H., Wittwer, C.T., 2004. Sensitivity and specificity of single-nucleotide polymorphism scanning by high-resolution melting analysis. Clin. Chem. 50, 1748–1754.
Reed, G.H., Kent, J.O., Wittwer, C.T., 2007. High-resolution DNA melting analysis for simple and efficient molecular diagnostics. Pharmacogenomics 8, 597–608.
Sauvage, C., Bierne, N., Lapegue, S., Boudry, P., 2007. Single nucleotide polymorphisms and their relationship to codon usage bias in the Pacific oyster *Crassostrea gigas*. Gene 406, 13–22.
Sauvage, C., Boudry, P., De Koning, D.J., Haley, C.S., Heurtebise, S., Lapègue, S., 2010. QTL for resistance to summer mortality and OsHV-1 load in the Pacific oyster (*Crassostrea gigas*). Anim. Genet. 41, 390–399.
Semagn, K., Bjørnstad, Å., Ndjiondjop, M.N., 2006. An overview of molecular marker methods for plants. Afr. J. Biotechnol. 5 (25), 2540–2568.
Shattuck-Eidens, D.M., Bell, R.N., Neuhausen, S.L., Helentjaris, T., 1990. DNA sequence variation within maize and melon: observations from polymerase chain reaction amplification and direct sequencing. Genetics 126, 207–217.
Shi, M., Lin, Y., Xu, G., Xie, L., Hu, X., Bao, Z., Zhang, R., 2013. Characterization of the Zhikong scallop (*Chlamys farreri*) mantle transcriptome and identification of biomineralization-related genes. Mar. Biotechnol. 15, 706–715.
Shi, Y., Wang, S., Gu, Z., Lv, J., Zhan, X., Yu, C., Bao, Z., Wang, A., 2014. High-density single nucleotide polymorphisms linkage and quantitative trait locus mapping of the pearl oyster, *Pinctada fucata martensii* dunker. Aquaculture 434, 376–384.
Small, K.S., Brudno, M., Hill, M.M., Sidow, A., 2007. Extreme genomic variation in a natural population. Proc. Natl. Acad. Sci. U. S. A. 104, 5698–5703.
Sodergren, E., Weinstock, G.M., Davidson, E.H., Cameron, R.A., Gibbs, R.A., Angerer, R.C., Angerer, L.M., Arnone, M.I., Burgess, D.R., Burke, R.D., 2006. The genome of the sea urchin Strongylocentrotus purpuratus. Science 314, 941–952.
Steine, G., Alfnes, F., RØRÅ, M.B., 2005. The effect of color on consumer WTP for farmed salmon. Mar. Resour. Econ. 20, 211–219.
Sun, X., Yang, A., Wu, B., Zhou, L., Liu, Z., 2015. Characterization of the mantle transcriptome of yesso scallop (*Patinopecten yessoensis*): identification of genes potentially involved in biomineralization and pigmentation. PLoS One 10, e0122967.
Van Ooijen, J.W., 2006. JoinMap 4.0, Software for the Calculation of Genetic Linkage Maps in Experimental Populations. Kyazma B. V., Wageningen, Netherlands.
Van Ooijen, J.W., 2009. MapQTL® 6.0, Sofware for the Mapping of Quantitative Trait Loci in Experimental Populations of Diploid Species. Kyazma B. V., Wageningen, Netherlands.
Venter, J.C., Adams, M.D., Myers, E.W., Li, P.W., Mural, R.J., Sutton, G.G., Smith, H.O., Yandell, M., Evans, C.A., Holt, R.A., 2001. The sequence of the human genome. Science 291, 1304–1351.
Voorrips, R., 2002. MapChart: software for the graphical presentation of linkage maps and QTLs. J. Hered. 93, 77–78.
Wan, S., Li, Q., Liu, T., Yu, H., Kong, L., 2017. Heritability estimates for shell color-related traits in the golden shell strain of Pacific oyster (*Crassostrea gigas*) using a molecular pedigree. Aquaculture 476, 65–71.
Wang, J., Li, Q., 2017. Characterization of novel EST-SNP markers and their association analysis with growth-related traits in the Pacific oyster *Crassostrea gigas*. Aquac. Int. 25, 1707–1719.
Wang, C.M., Zhu, Z.Y., Lo, L.C., Feng, F., Lin, G., Yang, W.T., Li, J., Yue, G.H., 2007. A microsatellite linkage map of Barramundi, *Lates calcarifer*. Genetics 175, 907–915.
Wang, C.M., Lo, L.C., Feng, F., Zhu, Z.Y., Yue, G.H., 2008. Identification and verification of QTL associated with growth traits in two genetic backgrounds of Barramundi (*Lates calcarifer*). Anim. Genet. 39, 34–39.
Wang, J., Qi, H., Li, L., Que, H., Wang, D., Zhang, G., 2015. Discovery and validation of genic single nucleotide polymorphisms in the Pacific oyster *Crassostrea gigas*. Mol. Ecol. Resour. 15, 123–135.
Wang, J., Li, L., Zhang, G., 2016. A High-density SNP Genetic Linkage Map and QTL Analysis of Growth-related Traits in a Hybrid Family of Oysters (*Crassostrea gigas* × *Crassostrea angulata*) Using Genotyping-by-sequencing. G3 (Bethesda). vol. 6. pp. 1417–1426.
Ward, R.D., English, L.J., McGoldrick, D.J., Maguire, G.B., Nell, J.A., Thompson, P.A., 2000. Genetic improvement of the Pacific oyster *Crassostrea gigas* (Thunberg) in Australia. Aquac. Res. 31, 35–44.
Wittwer, C.T., Reed, G.H., Gundry, C.N., Vandersteen, J.G., Pryor, R.J., 2003. High-resolution genotyping by amplicon melting analysis using LCGreen. Clin. Chem. 49, 853–860.
Xia, J.H., Liu, F., Zhu, Z.Y., Fu, J., Feng, J., Li, J., Yue, G.H., 2010. A consensus linkage map of the grass carp (*Ctenopharyngodon idella*) based on microsatellites and SNPs. BMC Genomics 11, 135.
Xiao, W., Oefner, P.J., 2001. Denaturing high-performance liquid chromatography: a review. Hum. Mutat. 17, 439–474.
Xu, L., Li, Q., Yu, H., Kong, L., 2017. Estimates of heritability for growth and shell color traits and their genetic correlations in the black shell strain of Pacific Oyster *Crassostrea gigas*. Mar. Biotechnol. 19, 421–429.
Yam, K.L., Papadakis, S.E., 2004. A simple digital imaging method for measuring and analyzing color of food surfaces. J. Food Eng. 61, 137–142.
Yan, Z., Fang, Z., Ma, Z., Deng, J., Li, S., Xie, L., Zhang, R., 2007. Biomineralization: functions of calmodulin-like protein in the shell formation of pearl oyster. Biochim. Biophys. Acta 1770, 1338–1344.
Yu, Z., Guo, X., 2003. Genetic linkage map of the eastern oyster *Crassostrea virginica* Gmelin. Biol. Bull. 204, 327–338.
Yu, Z., Guo, X., 2006. Identification and mapping of disease-resistance QTLs in the eastern oyster, *Crassostrea virginica* Gmelin. Aquaculture 254, 160–170.
Yue, G.H., 2014. Recent advances of genome mapping and marker-assisted selection in aquaculture. Fish Fish. 15, 376–396.
Yue, X., Nie, Q., Xiao, G., Liu, B., 2015. Transcriptome analysis of shell color-related genes in the clam *Meretrix meretrix*. Mar. Biotechnol. 17, 364–374.

Zhan, X., Wen, H., Shi, Y., Gu, Z., Wang, A., 2016. Association between novel EST-SNPs and commercial traits in *Pinctada fucata martensii*. Aquacult. Rep. 3, 209–213.

Zhang, G., Fang, X., Guo, X., Li, L., Luo, R., Xu, F., Yang, P., Zhang, L., Wang, X., Qi, H., Xiong, Z., Que, H., Xie, Y., Holland, P.W.H., Paps, J., Zhu, Y., Wu, F., Chen, Y., Wang, J., Peng, C., Meng, J., Yang, L., Liu, J., Wen, B.Z., Na, Z., Huang, Z., Zhu, Q., Feng, Y., Mount, A., Hedgecock, D., Xu, Z., Liu, Y., Domazet-Lošo, D., Du, Y., Sun, X., Zhang, S., Liu, B., Cheng, P., Jiang, X., Li, J., Fan, D., Wang, W., Fu, W., Wang, T., Wang, B., Zhang, J., Peng, Z., LI, Y., Li, N., Wang, J., Chen, M., He, Y., Tan, F., Song, X., Zhang, Q., Huang, R., Yang, H., Du, X., Chen, L., Yang, M., M, G.P., Wang, S., Luo, L., She, Z., MIng, Y., Huang, W., Zhang, S., Huang, B., Zhang, Y., Qu, T., Ni, P., Miao, G., Wang, J., Wang, Q., Steinberg, C.E.M., Wang, H., Li, N., Qian, L., Zhang, G., Li, Y., Yang, H., Liu, X., Wang, J., Yin, Y., Wang, J., 2012. The oyster genome reveals stress adaptation and complexity of shell formation. Nature 490, 49–54.

Zheng, X., Kuang, Y., Lv, W., Cao, D., Zhang, X., Li, C., Lu, C., Sun, X., 2013. A consensus linkage map of common carp (*Cyprinus carpio* L.) to compare the distribution and variation of QTLs associated with growth traits. Sci. China Life Sci. 56, 351–359.

Zhong, X., Li, Q., Yu, H., Kong, L., 2013. Development and validation of single-nucleotide polymorphism markers in the Pacific Oyster, *Crassostrea gigas*, using high-resolution melting analysis. J. World Aquacult. Soc. 44, 455–465.

Zhong, X., Li, Q., Guo, X., Yu, H., Kong, L., 2014a. QTL mapping for glycogen content and shell pigmentation in the Pacific oyster *Crassostrea gigas* using microsatellites and SNPs. Aquac. Int. 22, 1877–1889.

Zhong, X., Li, Q., Yu, H., Kong, L., 2014b. SNP mining in Crassostrea gigas EST data: transferability to four other Crassostrea species, phylogenetic inferences and outlier SNPs under selection. PLoS One 9, e108256.